ELSEVIER

Interfacial tension between magmatic sulfide and silicate liquids: Constraints on kinetics of sulfide liquation and sulfide migration through silicate rocks

James E. Mungall[a],*, Shanguo Su[a,b]

[a]Department of Geology, University of Toronto, 22 Russell St., Toronto, ON, Canada M5S 3B1
[b]China University of Geosciences, Beijing, China

Abstract

We have measured the interfacial tension γ_{SF} between sulfide and silicate melts over the temperature range from 1250 to 1325 °C by in situ measurement of the shapes of sessile drops of sulfide immersed in silicate melt, sitting upon level alumina substrates. The silicate melt was an alkali-free synthetic basaltic liquid. The sulfide melts were synthetic mixtures of Fe–Cu–Ni–S or Fe–S–O. The interfacial tension ranges from about 500 mJ m^{-2} for sulfide of FeS composition to approximately 600 mJ m^{-2} for sulfide containing 16 wt.% Cu or 6.5 wt.% Ni, and up to 650 mJ m^{-2} for Fe–S–O liquid containing 4 wt.% O. Contact angles vary from 150° to 180°, showing that sulfide liquid does not wet oxide minerals in silicate magmas. The density of sulfide melt does not depend strongly on Cu or Ni content, remaining between 4.0 and 4.5 g cm^{-3} over the range of Cu and Ni contents expected in sulfide magmas, but increases substantially to about 5.5 g cm^{-3} in Fe–S–O melts containing 4 wt.% O. Our results can be combined with conventional concepts of nucleation theory to indicate that when silicate magmas exist at small degrees of supersaturation, sulfide drops may nucleate rarely and at widely spaced intervals, leading to kinetic control of the compositions of the resulting droplets. In light of our results, we use simple scaling arguments to argue that sulfide magmas are not capable of migrating through partially molten silicate rocks by capillary forces alone, but may be forced through narrow grain boundaries or grain edges only by the flow of the enclosing silicate melt. During melt extraction by compaction of partially molten mantle peridotite, it is highly unlikely that silicate flow rates could be sufficiently rapid to permit the entrainment of droplets of sulfide liquid. At temperatures below the solidus of enclosing silicate rocks, sulfide melt will be free to travel along fractures or grain boundaries. The mobility of sulfide melts through completely solidified silicate rocks may account for the widespread observation that late-stage, highly fractionated sulfide liquids have escaped from cooling bodies of massive sulfide to form veins and disseminations of Cu-rich sulfide minerals in their silicate host rocks.
© 2005 Elsevier B.V. All rights reserved.

* Corresponding author. Fax: +1 416 978 3988.
  E-mail address: mungall@geology.utoronto.ca (J.E. Mungall).

1. Introduction

The energy of formation of surfaces between thermodynamically distinct phases, also known as interfacial tension, plays a major role in controlling kinetics of reactions and the textures that are formed in magmatic systems. The rates and directions of dynamic processes such as nucleation and growth of new phases are strongly affected by surface processes. In a recent paper, we suggested that large sulfide-silicate interfacial tensions might serve to inhibit the nucleation of sulfide drops within silicate melts, allowing substantial metastable supersaturation in sulfide to occur and affecting the number density of sulfide droplets [1]. These phenomena will, in turn, affect the compositions of sulfide liquids that may accumulate to form ore deposits in magmatic systems. The interfacial tension of sulfide–silicate liquid interfaces has only previously been measured in metallurgical matte–slag systems [2,3] whose compositions differ markedly from natural sulfide and silicate magmas. In this contribution, we describe the results of a series of experiments conducted using the sessile drop technique to determine the sulfide–silicate surface tension over a wide range of sulfide melt compositions and temperatures in a synthetic silicate melt. We use the results to put some constraints on the nucleation kinetics of sulfide liquids in basaltic magmas and on the wetting behavior of sulfide liquids against solids in the presence of silicate melts.

2. Previous work

Previous studies using the sessile drop method [2,3] have focussed on metallurgical slag–matte systems containing extremely iron-rich, silica-undersaturated slags similar to fayalite in bulk composition, and extremely Cu- and Ni-rich mattes lacking in oxygen. The results of these slag–matte studies can be summarized as follows.

The interfacial tension between iron-rich slag and iron-rich sulfide at 1200 °C is of the order of 300 mJ m^{-2}, but it increases to values exceeding 450 mJ m^{-2} as the proportion of Ni and increases to 100% [2]. The contact angle remains fairly constant near 170° regardless of matte or oxide substrate composition. Densities of the sulfide liquids vary from about 4.0 g cm^{-3} for pure FeS liquid to slightly above 5 g cm^{-3} for both Cu$_2$S and Ni and liquids. Over the temperature range from 1000 to 1300 °C, as the interfacial tension decreased about 10%, sulfide liquid density decreased by only about 0.2 g cm^{-3} [3].

3. Experimental approach

3.1. Technique

We used sessile drop technique to measure interfacial tension between sulfide and silicate melts. The following is a brief summary of the method used; a detailed description of the equipment and protocols was presented elsewhere [2]. Synthetic Fe–Ni–Cu–S or Fe–S–O liquids were immersed in synthetic basaltic melt in alumina crucibles in a vertical MoSi$_2$ resistance furnace and heated under an inert Ar atmosphere to temperatures from 1250 to 1325 °C (Fig. 1). In each experiment, the sulfide formed a single drop in the bottom of the crucible, which was imaged in situ using a X-ray generator and medical X-ray film. Use of this in situ technique allows direct measurement at run conditions of the shape of the drop, which is a sensitive function of the melt densities and of the interfacial energy of the surface separating them.

Temperature was controlled with a Pt–Pt$_{87}$Rh$_{13}$ thermocouple. Chips of sulfide matte starting material weighing about 0.7 g and chips of silicate glass totalling about 2 g were placed in the alumina crucible which was then placed on a refractory stand inside the alumina furnace tube. To prevent oxidation of the sulfide, the furnace tube was alternately evacuated to 0.1 mm Hg vacuum and flushed with high-purity Ar (99.999%) three times. During the subsequent run, high-purity Ar was slowly passed through the furnace to ensure that air was excluded.

Charges were heated to run temperature over periods of about 1 h and held at 1250 °C for 10 min before the first images were taken. Previous time series experiments have shown that this is more than enough time to allow the sessile drop to reach a shape dictated by the force balance at equilibrium [2]. The progress of
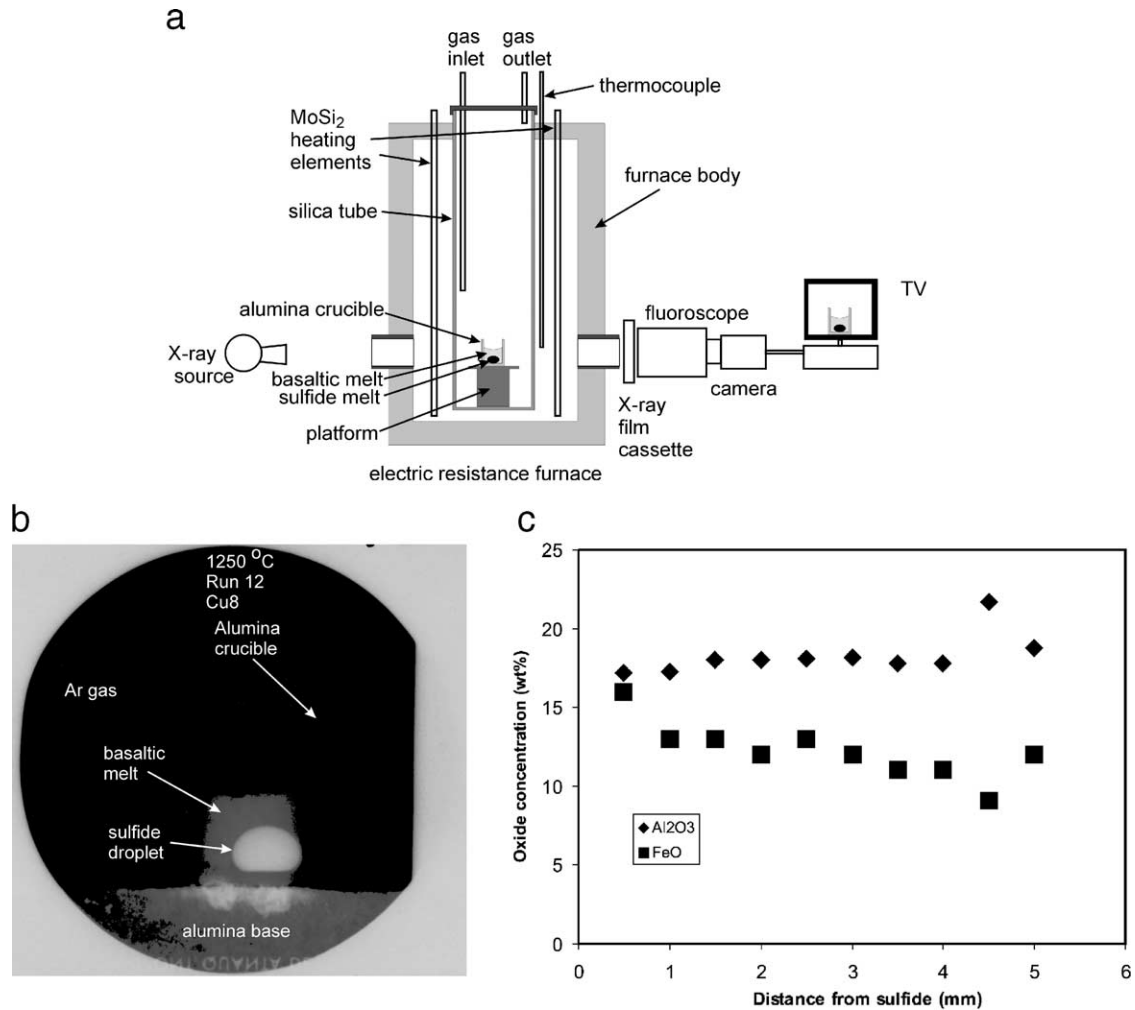
Fig. 1. (a) Experimental apparatus for in situ determination of contact angle by X-ray imaging. (b) Typical X-radiograph of a sulfide droplet imaged in situ at 1250 °C. This sulfide liquid contained 8 wt.% Cu (Run 12 in Table 1). (c) FeO content of silicate glass from Experiment 24, along a horizontal traverse from the sulfide droplet at left to the outer wall of the crucible at right. FeO has been transferred from the sulfide to the silicate in this experiment. In experiments not containing O in the sulfide, we do not observe compositional gradients within the silicate glass.

the experiment was monitored in real time using a video camera and VCR, whereas high-resolution images for data reduction were taken using medical X-ray film with a resolution of 30 pixels/mm. The X-ray images were exposed for 1 s at 70 kV. Subsequent ramps to higher temperatures were followed by 10-min soaks to ensure that droplets had reached a stable form before being imaged. The temperatures at which droplets were imaged are listed in Table 1. In each experiment, a single droplet of sulfide was imaged

several times at different temperatures over the course of several hours.

3.2. Synthesis

Sulfide matte in the system Fe–Ni–Cu–S was synthesized by mixing FeS (Fisher Scientific), Cu_2S (INCO Ltd, Missisauga, ON), and Ni_3S_2 (Ventron, Danvers MA) powders into an alumina crucible and heating the mixture under an Ar atmosphere for 40

Table 1
Run conditions, nominal and measured sulfide liquid compositions

Run	Fe	Cu	Ni	S	O
Composition: nominal (wt.%)					
31	63.53	0.00	0.00	36.47	0.00
13	60.35	3.99	0.00	35.66	0.00
12	57.17	7.99	0.00	34.84	0.00
11	54.00	11.98	0.00	34.03	0.00
10	50.82	15.97	0.00	33.21	0.00
18	60.35	0.00	3.26	35.99	0.00
20	54.00	7.99	3.26	34.35	0.00
19	47.64	15.97	3.26	32.72	0.00
27	57.17	0.00	6.52	35.50	0.00
16	50.82	7.99	6.52	33.86	0.00
15	44.47	15.97	6.52	32.23	0.00
28	44.47	3.99	16.29	33.21	0.00
Composition: measured (wt.%)					
22	64.22	–	–	33.59	2.18
24	64.72	–	–	31.55	3.73

min at 1325 °C. The furnace was then turned off and allowed to cool to about 100 °C over about 1 h before the crucible was removed. The compositions of the Fe–Ni–Cu–S mattes prepared in this way are given in Table 1.

Sulfide matte in the system Fe–S–O was prepared by mixing Fe_2O_3, Fe and FeS obtained from Fisher Scientific into an alumina crucible and fusing the mixture as described above for 50 min under Ar. The nominal compositions of the Fe–Ni–Cu–S–O liquids used in our experiments are given in Table 1.

A synthetic basaltic glass was prepared in a similar fashion. Powders of SiO_2, Al_2O_3, Fe_2O_3, MgO and CaO (Fisher Scientific) were mixed and fused in a Pt crucible for 4 h at 1400 °C. The melt was quenched to glass by removing the crucible from the furnace and allowing it to cool in air, after which the glass was broken out of the crucible. The nominal composition (as weighed in) of the resulting glass is 51.47% SiO_2, 16.29% Al_2O_3, 10.35% Fe_2O_3, 9.95% MgO, and 11.95% CaO. In early attempts, we used a silicate melt containing Na_2O and K_2O but encountered difficulties with foaming when the alkali-bearing melts were placed in contact with the sulfide liquid during the heating stage of the experiments. We therefore did all subsequent experiments using the simplified alkali-free synthetic basalt composition listed above. Since the principal control on interfacial tension is expected to be the difference in gross melt structure between

liquids whose dominant anions are sulfur or oxygen, we do not anticipate that the absence of alkali cations from our experiments would have a significant effect on the measured values.

4. Results

4.1. Compositions

After experiments were complete, we mounted the cooled crucibles in epoxy before sectioning and polishing them. The sulfide crystallized during cooling to a fine trellis-textured intergrowth of monosulfide solid solution (mss) and Cu- and Ni-rich phases in the Fe–Ni–Cu–S experiments or magnetite and mss in the Fe–S–O experiments.

We were unable to design an experiment in which all of the materials would be in equilibrium. A metal substrate would react with the sulfide melt, whereas the alumina substrate we chose was inert with respect to the sulfide but reacted slowly with the silicate melt, so there were inevitably some compositional gradients in the silicate melt. Although the composition of the silicate melt may have been slightly inhomogeneous, we assume that its composition at the silicate–sulfide interface was in local equilibrium with the sulfide melt. This inhomogeneity is tolerable in the present context because only the interfacial compositions and the bulk densities of the two melts will dictate the stable form of a sessile drop. The direct effects of compositional gradients on effective interfacial tension are expected to be unmeasurably small after several minutes [6], and we therefore accept their inevitable presence.

Inspection of the cooled experimental charges shows that there was undoubtedly some reaction between the sulfide liquid and the silicate melt, as evidenced by the presence of wisps and streamers of visibly different composition within the quenched glass near its interface with the quenched sulfide. The solubility of sulfide liquid in basaltic melts is sufficiently low (of the order 1000 ppm [4]) that the compositional change could not have been extreme in either of the two immiscible liquid reservoirs. Transfer of Cu or Ni to the synthetic basaltic melt is exceedingly unlikely given the highly chalcophile nature of these two metals [5]. We analysed of the products of

two of the experiments done using Fe–Ni–Cu–S liquids and synthetic basalt to assess the extent of reaction between the sulfide melt, the silicate melt, and the alumina crucible. The electron microprobe was used to analyse the silicate glass left after cooling of the charges, along horizontal and vertical traverses running away from the sulfide globule to the wall of the crucible and to the top of the glass meniscus. In experiments not involving O, there was no significant change in glass composition along either horizontal or vertical traverses, even for Al_2O_3. This is probably due to the formation of crystals of spinel on the melt–alumina contact, which armored the interface and caused the rate-limiting step in alumina transfer to the melt to be solid state diffusion of Al_2O_3 within the spinel. In the product of experiment 24, the vertical traverse showed no compositional variation but the horizontal one revealed that the silicate glass had taken up an additional 7.5 wt.% FeO at the boundary with the sulfide, as shown in Fig. 1c. This is in agreement with our observation (below) that in the experiments with the highest nominal FeO content in sulfide, the measured FeO content of the sulfide was considerably less than anticipated due to loss of FeO from the sulfide to the silicate. In light of these observations, we have discarded the results of the experiment with nominal O concentrations in sulfide exceeding 4 wt.%.

The existence of disequilibrium between substrate and liquid, or between the two liquids, does not preclude the measurement of a valid interfacial tension, for the following reasons. The timescale at which the sessile drop will assume the form that minimizes its surface free energy depends on the viscous relaxation time of both melts. Since the viscosity of molten basalt at our run temperatures is on the order of 100 Pa s, and the elastic shear modulus G of the melt is approximately 3×10^{10} Pa, we can use the Maxwell relation [6] to estimate the viscous relaxation time of the basaltic liquid at approximately 3×10^{-9} s. Viscous flow of the basalt and sulfide melt to a stable shape minimizing the local free energy of the interfacial region will therefore occur over periods of seconds or less, whereas the diffusive re-equilibration of the melts and solids will take place on timescales of minutes or hours. The measured shapes of sessile sulfide drops therefore reflect the energy balance dictated by

the interface compositions rather than the bulk compositions of the melts.

We had some concerns about possible oxygen loss from the Fe–S–O mattes either during synthesis or during heating to experimental run conditions and therefore assessed the compositions of the cooled sulfide melts after experiments were complete. This was done by photographing the polished matte surface and using image analysis software to calculate the modal proportions of mss and magnetite (identified by reflected light petrography and electron microprobe analysis). The compositions estimated by image analysis are compared with the nominal compositions in Table 1; the correspondence is quite close for the runs with nominal O contents of 2 and 4 wt.% and indicates that oxygen loss did not affect our results in a significant way in these runs. In the run nominally containing 8% O, we measured only 3.7% O, indicating that O was lost from the original sulfide mixture to the basaltic melt, perhaps accommodated within the basaltic melt by participation in the homogeneous equilibrium $2FeO + 0.5 \ O_2 = Fe_2O_3$, or perhaps escaping into the furnace atmosphere during the initial melting of the sulfide and silicate during the heating stage of the experiment. Since the resulting O concentration was only about 4 wt.%, we have discarded the results from both the 6% and 8% O runs.

4.2. Measurement of interfacial tension

If a droplet of Fe–sulfide liquid is immersed in silicate liquid and sits at rest on a smooth, level alumina surface, then it will have an axisymmetric form as shown in Fig. 2, and the angle θ between the
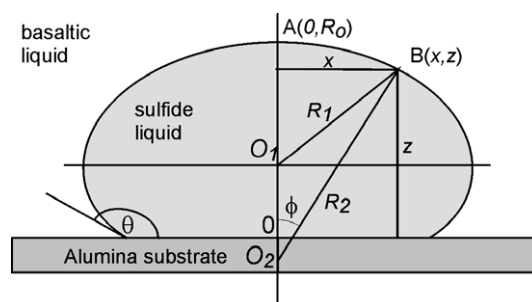

Fig. 2. (a) Cross-sectional view of a sessile drop illustrating the contact angle and geometrical parameters used to determine interfacial tension.

sulfide–silicate interface and the alumina substrate will be given by Young's equation:

$$\gamma_{SF}\cos\theta = \gamma_{AS} - \gamma_{AF} \tag{1}$$

where γ is the interfacial tension between two subscripted phases and the subscripts S, F, and A denote silicate liquid, Fe–sulfide liquid, and alumina, respectively [7]. The drop's equilibrium shape will be determined by the Laplace equation

$$\Delta P = \gamma_{SF}\left(\frac{1}{R_1} + \frac{1}{R_2}\right) \tag{2}$$

where ΔP is the pressure difference across the interface at point B, γ_{SF} is the interfacial tension, and R_1 and R_2 are the principal radii of curvature of the drop [7]. The pressure change ΔP across the interface also depends upon the density difference between the two liquids ($\Delta\rho$), the acceleration due to gravity g and the height h of the liquid column above the point of interest

$$\Delta P = \rho g h \tag{3}$$

Eqs. (1)-(3) may be combined to obtain the Bashforth–Adams equation:

$$\frac{1}{R_1/R_0} + \frac{\sin\phi}{x/R_0} = 2 + \frac{(\Delta\rho)gR_0^2}{\gamma_{SF}} \cdot \frac{z}{R_0} \tag{4}$$

where R_1 and R_0 are radii of curvature of the drop at points B and A, respectively, x and z are the horizontal radius and height of point B above the datum, and ϕ is the angle between R_2 and the axis of symmetry of the drop [8].

Eq. (4) was implemented by scanning X-radiographs of the experiments and extracting Cartesian coordinates (x,z) of points around the perimeters of the drops. Knowing the weight of the drop as measured by weighing the matte chip before the experiment, we calculated its density from its cross-sectional area and thus solved for γ_{SF} at each point B around the margin of the drop using a computer program by Rotenberg [8].

4.3. Controls on interfacial tension

The values of interfacial tension extracted from the X-radiographs using the Bashforth–Adams equation are given in Table 2. All of the interfacial tensions measured are in the range from 500 to 700 mJ m^{-2}. As shown in Fig. 3, γ_{SF} shows no discernable dependence on temperature over the range from 1225 to 1325 °C for any composition except Cu16 and Ni6. We assume, therefore, that the variation in γ_{SF} with temperature is random and that the apparent trends shown by Cu16 and Ni6 are purely due to chance. The observation that the temperature dependence is less than the precision of the measurements is not surprising, considering that γ_{SF} will not drop to zero until the temperature at which sulfide and silicate liquid becomes completely miscible. Although the solubility of sulfide in silicate melt does increase slightly with increasing temperature, it remains extremely low even at 1400 °C [4], so we should not expect to see any appreciable change in γ_{SF} over the range of temperatures at which we worked. Because the images for each experiment were taken after ramping from one temperature to another and then holding for several minutes at each temperature, over a total period of several hours for each composition, and because there are no discernable effects of temperature itself on droplet shape, the group of images for each run can be taken as a time series and therefore indicate the precision and reproducibility of our data. In Table 2, we list the mean and standard deviation (σ) of γ_{SF} as measured for each sulfide melt composition over a range of temperatures; these standard deviations are used to establish the magnitude of lσ error bars in subsequent figures.

The dependence of γ_{SF} on oxygen, Cu and Ni contents of the sulfide liquids is shown in Fig. 4. Data for experiments in which both Cu and Ni were added are presented in Table 2 but not shown in Fig. 4. The data are plotted for each composition as the mean of several determinations at different temperatures, with error bars extending to one standard deviation above and below the average calculated individually for each composition. The addition of other components to melts of FeS composition leads to small but probably significant increases in γ_{SF}. The intensity of this effect is similar for Ni and Cu. In each case, the total increase in γ_{SF} is about 20%, from approximately 540 mJ m^{-2} in pure FeS to about 620 mJ m^{-2} for the addition of 6.5 wt.% Ni or 16 wt.% Cu. The addition of up to 3.9% O has had no significant effect on YSF; the effects of larger additions of O cannot be

Table 2
Measured interfacial angles, interfacial energies, and melt densities

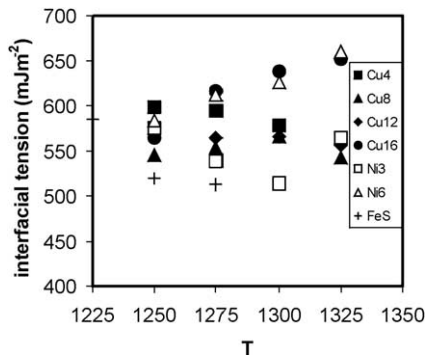| Run	1250			1275			1300			1325			Mean γ_{SF} (mJ m^{-2})	Standard deviation of γ_{SF} (mJ m^{-2})	Mean ρ (g cm^{-3})	Standard deviation of ρ (g cm^{-3})
	θ (°)	γ_{SF} (mJ m^{-2})	ρ (g cm^{-3})	θ (°)	γ_{SF} (J m^{-2})	ρ (g cm^{-3})	θ (°)	γ_{SF} (mJ m^{-2})	ρ (g cm^{-3})	θ (°)	γ_{SF} (mJ m^{-2})	ρ (g cm^{-3})				
31	168	519	4.42	157	512	4.56	×	×	×	×	×	×	539	40.3	4.57	0.16
13	168	598	4.32	161	594	4.18	155	578	4.26	×	×	×	590	10.6	4.25	0.07
12	170	545	4.23	164	554	4.21	161	566	4.29	164	543	4.09	552	10.5	4.21	0.08
11	167	577	4.27	173	565	4.2	164	566	4.32	168	556	4.38	566	8.6	4.29	0.08
10	172	564	4.65	178	617	4.68	160	638	4.84	169	652	4.67	618	38.6	4.71	0.09
18	167	575	4.03	163	539	4.1	176	514	4.1	167	564	4.11	548	27.2	4.09	0.04
20	166	532	3.96	180	532	3.9	180	547	3.9	180	539	3.91	538	7.14	3.92	0.03
19	165	505	4.76	×	×	×	×	×	×	165	505	4.76	505	−	4.76	−
27	166	584	3.86	166	613	4	175	626	4.35	175	660	3.93	621	31.5	4.04	0.22
16	161	520	4.3	×	×	×	170	512	4.19	×	×	×	516	5.7	425	0.08
15	167	573	4.29	×	×	×	×	×	×	167	573	4.29	573	−	4.29	−
28	157	545	4.11	165	555	4.22	159	572	4.13	168	527	4.11	550	18.8	4.14	0.05
22	165	546	4.12	166	546	4.12	178	538	4.02	180	498	4.00	532	23.0	4.07	0.06
24		×	×	151	663	5.51	161	640	5.57	158	653	5.68	652	11.5	5.59	0.09

Fig. 3. Dependence of interfacial tension on temperature. Numbers in the legend refer to the nominal concentration of metal in the sulfide liquid, e.g., Run Ni3 contained 3.26 wt.% Ni.

addressed because of our observations of extensive FeO exchange between the sulfide and silicate melts. Overall, we observe sulfide–basalt interfacial tensions of approximately 600 ± 50 mJ m^{-2} regardless of temperature or sulfide liquid composition.

The results of our experiments can be used to place approximate constraints on the wetting angle of sulfide liquid against an oxide mineral (i.e., alumina) when both are immersed in basaltic silicate melt and also give preliminary data concerning the density of sulfide liquid as function of temperature and sulfide melt composition. Fig. 5 illustrates the relation between wetting angle θ and the amounts of Cu, Ni or O present in the melt. There appears to be no significant variation in θ with any of these compositional parameters, although there is a suggestion that O increases with increasing amounts of Cu and Ni but decreases with the addition of oxygen. It is also noteworthy that in the experiment conducted with 8% Cu and 3.26% Ni, the wetting angle was 180° over the temperature range from 1275 to 1325 °C, meaning that the sulfide drop remained completely immersed in the silicate liquid, being separated from the solid substrate at all times by a thin film of silicate melt.

As shown in Fig. 6, the density of sulfide liquid is generally between 4 and 4.5 g cm^{-3}. The addition of small amounts of Cu, Ni or O apparently causes a slight decrease in density relative to pure FeS melt. Addition of larger amounts of Cu or Ni causes moderate increases in density such that the most Cu- or Ni-rich sulfide melts have approximately the same density as the FeS melt, close to 4.5 g cm^{-3}. The

addition of 4% O to FeS melt causes an increase in melt density of approximately 30%, to values near 5.5 g cm^{-3}. This observation is in keeping with the much smaller ionic radius of oxygen compared with that of S. The effect of temperature on sulfide melt density appears to be minimal.
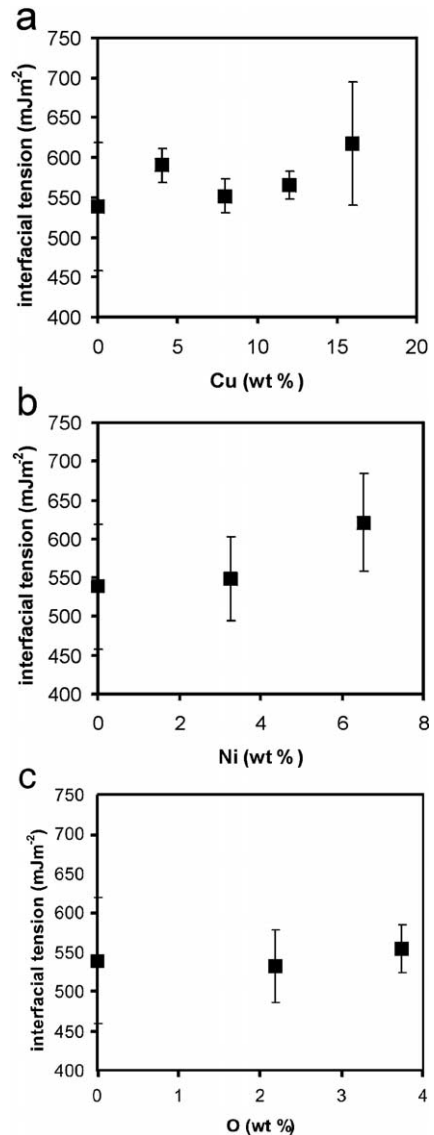

Fig. 4. Dependence of interfacial tension on sulfide melt composition. (a) γ_{SV} vs. Cu concentration, oxygen-free. (b) γ_{SV} vs. Ni concentration, oxygen-free. (c) γ_{SV} vs. O concentration. Error bars in this and all subsequent figures show the range of two times the standard deviation.
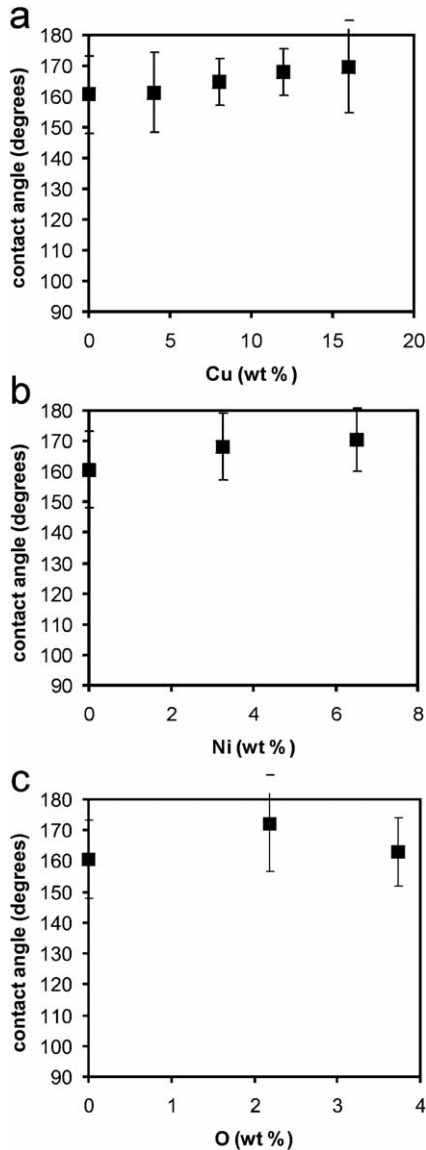
Fig. 5. Dependence of contact angle on sulfide melt composition. (a) θ vs. Cu concentration, oxygen-free. (b) θ vs. Ni concentration, oxygen-free. (c) θ vs. O concentration.

sulfide melt composition are minor, causing variations to values not larger than about 700 mJ m^{-2} over the range of sulfide melt compositions anticipated in natural systems. These values are considerably higher than the values of 300–450 mJ m^{-2} previously recorded for synthetic slag–matte systems [2,3], probably because the slags previously studied con-
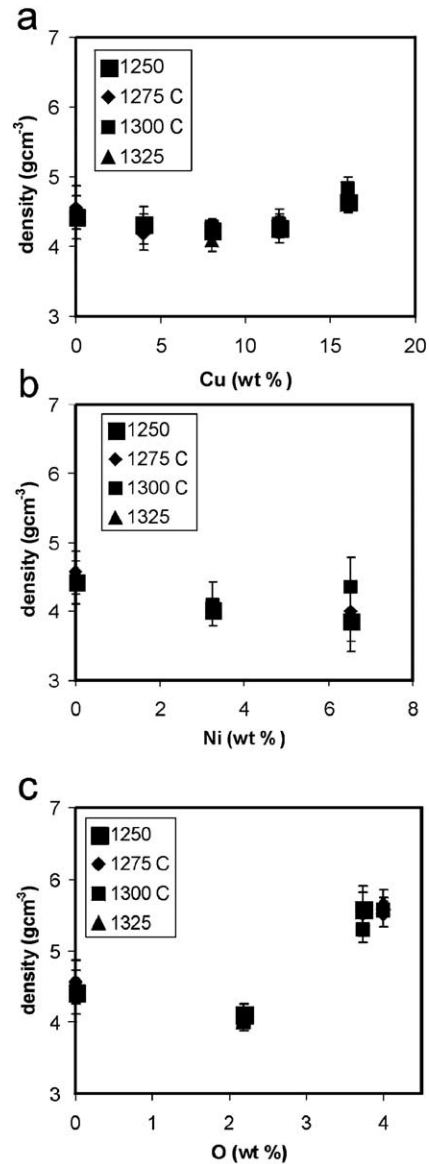

Fig. 6. Dependence of sulfide melt density on composition. (a) ρ vs. Cu concentration, oxygen-free. (b) ρ vs. Ni concentration, oxygen-free. (c) ρ vs. O concentration.

The first-order results of our study can therefore be summarized as follows. The measurement of interfacial tension by the in situ measurement of sessile drop shape using X-radiography has an inherent precision of about between 10% and 20%, allowing estimation of the interfacial tension in basalt–sulfide systems of the order of 600 ± 100 mJ m^{-2} with no evident dependence on temperature. The effects of

tained approximately 50% FeO and were therefore much more similar to sulfide melts than the present synthetic basalt.

5. Discussion

5.1. Nucleation of sulfide droplets

The nucleation and growth of a sulfide drop as a new phase in a silicate melt depends on several factors. The sulfide drop, once formed, must be in equilibrium with the host melt, that is, the system must at least be saturated with sulfide. The following discussion of nucleation kinetics recapitulates the standard treatment of Gibbs' classical thermodynamic theory of heterogeneous systems [9,10]. The total energy ΔG of a newly formed nucleus of sulfide melt is the sum of its internal energy and its surface energy,

$$\Delta G = \frac{4}{3}\pi r^3 \frac{\Delta G_F}{V_m} + 4\pi r^2 \gamma_{SF} \tag{5}$$

where ΔG_F is the free energy per mole of sulfide melt, r is the droplet radius, V_m is the molar volume of sulfide melt, and γ_F is interfacial tension as defined above.

For large droplets, the second term in Eq. (5) is negligible, and the total energy of the droplet simply depends on its volume and its free energy per unit volume. In other words, the usual macroscopic equilibrium thermodynamic approach will successfully predict whether or not a droplet can exist. However, before droplets can grow to sufficient size to justify neglecting the surface term in Eq. (5), they must nucleate and grow past a critical radius at which the sum of the surface term and the volume term reaches its maximum value. Eq. (5) can be differentiated with respect to droplet radius to find the critical radius at which $d\Delta G_c/dr = 0$:

$$r_c = \frac{-2\gamma_{SF}V_m}{\Delta G_c} \tag{6}$$

Any droplet smaller than the critical radius will have a greater total free energy than an equivalent system not containing a drop and will therefore tend to shrink, whereas droplets larger than the critical radius will be able to minimize their total free energy by growing. Substituting the critical radius r back into Eq. (5)

gives the free energy ΔG_α of a nucleus at its maximum value

$$\Delta G_\alpha = \frac{16\pi\gamma_{SF}^3 V_m^2}{3\Delta G_F^2} \tag{7}$$

The free energy of the droplet at its critical radius corresponds to the activation energy for nucleation of the droplet. The rate of formation R_o of supercritical nuclei in a unit volume of the melt per unit time is given by

$$R_o = K\exp\left\{\frac{-\Delta G_\alpha}{RT}\right\} \tag{8}$$

The pre-exponential factor K contains information about the frequency of appearance of incipient droplet nuclei, R is the ideal gas constant and T is absolute temperature. The role of interfacial tension in controlling droplet nucleation can be seen by considering the contribution Eq. (7) makes to Eq. (8). Because γ_{SF} is raised to the third power in Eq. (7), small increases in γ_{SF} can lead to extreme increases in the activation energy of formation of sulfide droplets, with a consequent radical decrease in the number density of nucleation sites in the silicate magma. The competing thermodynamic force is provided by the amount by which the free energy of the bulk system is reduced by the formation of a separate sulfide phase. As the degree of sulfide supersaturation increases, the energetic penalty to the system incurred by nucleation of sulfide droplets decreases in magnitude, the activation energy of formation of droplets decreases, and nucleation is enhanced.

The controls on homogeneous nucleation of silicate and oxide minerals from silicate magmas are essentially identical to those summarized above for sulfide drops. In general, phases with small interfacial energies will tend to nucleate rapidly and at small degrees of supersaturation. Surface energies of silicate minerals in silicate melt are of the order of 120 mJ m^{-2} [11,12], about one-fifth that measured here for sulfide–silicate interfaces. The activation energy hindering nucleation of sulfide melt from silicate magma will therefore be approximately two orders of magnitude (i.e., 5^3) greater than that of silicate mineral nucleation, and sulfide liquation will therefore tend to lag substantially behind that of silicate crystals at small degrees of sulfide supersaturation.

Whereas heterogeneous nucleation on preexisting phases may offer a shortcut to nucleation for phases such as silicate minerals, this avenue is not open to sulfide melt in a magma containing only silicate melt and silicate or oxide crystals. This can be seen through consideration of Eq. (1) and the very large contact angles measured in this study, which show that the surface energy of sulfide–solid interfaces is even higher than that of the sulfide–silicate melt interface.

If a sulfide-undersaturated silicate magma is evolving by fractional removal of silicate minerals as it cools, S will become enriched in the residual melt to the point at which sulfide liquid reaches saturation. The results of our study, combined with the theoretical considerations described above, indicate that sulfide droplets may be unable to nucleate for some time after the system has evolved to the point of equilibrium sulfide saturation. When sulfide droplets do eventually form, they will do so at widely spaced sites due to the infrequency of nucleation events, and they may be able to grow to sufficient size to settle to the base of the magma chamber while the silicate melt around them remains in a state of sulfide supersaturation. The consequences of such behavior have recently been explored [1] and will not be reiterated here in detail. In brief, this phenomenon should result in the deposition of sulfide droplets whose compositions are entirely controlled by kinetic factors and by the small degree of supersaturation of sulfide rather than by equilibrium partitioning of metals and sulfur between the coexisting silicate and sulfide melts. Sulfide droplets formed at small degrees of supersaturation form at very large silicate/sulfide mass ratios, leading to the deposition of sulfide cumulates containing very high tenors of highly chalcophile elements.

5.2. Sulfide infiltration of silicate rocks

Sulfide liquid is sometimes inferred to have migrated through solid or semi-solid silicate rocks. The results of this process are commonly observed as fine disseminations of sulfide minerals around sharp-edged magmatic sulfide veins, particularly those veins injected at relatively low temperatures from highly evolved Cu-rich sulfide magmas. On a larger scale, it has recently been proposed that sulfide liquids can migrate distances of tens or even hundreds of meters through partially solidified cumulate piles at Sudbury

[13] and in the Bushveld intrusion [14]. Furthermore, it has recently been suggested that extraction of basaltic melt from partially melted peridotite in the upper mantle could be accompanied by entrainment of undissolved immiscible sulfide melt droplets [15]. If this was the case, then estimates of basaltic melt composition based upon models of equilibrium partitioning between melt and restite (including sulfide melt) would be invalidated and we would have no means to predict the behaviour of chalcophile elements in such systems.

Two general circumstances can apply to the problem of sulfide migration in solid or semi-solid silicate rocks. If the enclosing silicate rock is completely solid, then the distribution of sulfide melt among the silicate crystals will depend on the wetting properties of sulfide liquid against the solids. If the dihedral angle between crystal faces abutting a pore filled with sulfide melt is less than $60°$, the sulfide liquid will completely penetrate triple grain boundaries even at vanishingly small proportions of sulfide liquid in the bulk system [16]. Measured dihedral angles for sulfide liquids against a variety of common silicate and oxide minerals show a strong dependence on composition of both the silicates and the sulfide liquid, being lowest for those compositions richest in FeO and in contact with chromite crystals [17–21]. Sulfide liquid may be wetting or non-wetting and, in many cases, will be able to penetrate considerable distances through completely solid silicate rocks in a process driven entirely by capillary forces.

If the enclosing silicate rock retains some silicate melt between the solid crystals, then the sulfide melt will form discrete droplets. Where these droplets are in contact with solids, they will wet them very little or not at all, given that their contact angles are expected to be on the order of $160–180°$. Droplets with contact angles of $160°$ will not be able to penetrate openings that are already there, let alone generate new openings by capillary forces. It is therefore exceedingly difficult for sulfide liquid to migrate through semi-solid silicate rocks as long as residual traces of silicate melt remain.

The extraction of silicate melt from semi-solid cumulates or partially molten upper mantle peridotite occurs primarily by compaction of the solid framework and expulsion of the melt by porous flow between the solid grains [22,23]. Due to their comparatively high viscosities, silicate melts may

entrain sulfide drops and carry them along [13,15]. The feasibility of this process depends on the balance between the viscous force in the silicate melt that tends to push the sulfide drops into small cavities, and surface tension in the sulfide drop that tends to restore it to a spherical shape and retard its entrance into a small cavity. The magnitude of the viscous force depends on the rate of flow of the silicate melt as well as the melt viscosity, which itself is a strong function of temperature and composition. There will therefore be a range of conditions under which sulfide is forced to migrate through a silicate rock by the flow of silicate melt, and other conditions under which sulfide is trapped in the larger interstitial volumes while silicate melt is free to migrate around it. The transition between these two types of behaviour will be sensitive to sulfide drop size, sulfide melt fraction, grain size of the silicate rock, the wetting angle of silicate melt against the silicate or oxide minerals, and the tortuosity of the channels linking larger melt volumes [24].

A detailed analysis of the physics of the transport of two immiscible liquids through a porous medium is beyond the scope of this article, but we can make some simple first-order statements. Since the interfacial tension between sulfide melt and silicate melt is rather large, there is a large energetic penalty for the existence of large numbers of small droplets, as discussed above. Therefore, given time to reach equilibrium, small droplets will shrink and large droplets will tend to assume the maximum size that permits them to reside as spheres in pores at four-grain contact points as shown in Fig. 7a. Since the four-grain contact points in a texturally mature peridotite are invariably larger than the pore throats along three-grain boundaries, it follows that sulfide drops will always grow to a size at which they are just in contact with the walls of the four-grain contact points. The timescale for attainment of this kind of textural maturity in a partially molten rock depends on the diffusivity of the melt components in the intergrain melt and the distance between pores. If the grain size x is of order 1 mm, and chemical diffusivities D of the components of a basaltic melt at 1400 °C are about 10^{-7} cm^2 s^{-1}, then the time required for the development of a mature texture will be on the order of x^2/D, i.e., 10^5 s. This is a much
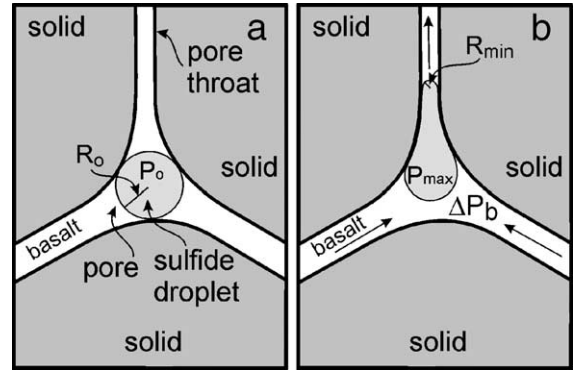

Fig. 7. Schematic illustration of a sulfide droplet being forced through a narrow pore in a partially molten silicate rock. (a) The system at rest. The sulfide drop will tend to fill the pore, growing at the expense of smaller droplets in neighboring pores, until it reaches the size permitting it to touch the pore walls while remaining spherical. (b) During flow of basaltic melt through the pore throats, the hydraulic gradient in the basalt between one pore and the next must be equal to or larger than the capillary pressure imposed by reducing the radius of curvature of the droplet as it passes through the pore throat before the sulfide droplet can be forced through to the next pore.

longer time than the duration of the recent experiments which purport to demonstrate the longevity of small sulfide droplets [15], but much shorter than the timescale of melt extraction from a parcel of melting peridotite, which may spend several million years in an ascending melt column in the asthenosphere under a mid-ocean spreading center or plume head.

As a single sulfide droplet is pressed against a single cylindrical pore throat by the flow of basaltic melt during compaction-driven melt extraction, its ability to enter the pore throat will depend on the balance of two forces. The pressure within the droplet rises as a function of the radius of curvature of the largest spherical cap that can pass through the pore throat, as shown by Eq. (2). Neglecting the effects of gravity on pressure within the droplet, the pressure everywhere within the drop will be equal. Setting the capillary pressure within the droplet in its equilibrium spherical form to be P_o, and the pressure within the droplet when part of it is constricted to be P_{max}, we can see that the pressure within the droplet will be larger than the equilibrium value by an amount ΔP when its leading edge reaches the pore throat:

$$\Delta P = P_{max} - P_o = \frac{2\gamma_{SF}}{R_{min}} - \frac{2\gamma_{SF}}{R_o} \qquad (9)$$

The droplet cannot be forced through the pore throat unless this excess pressure is opposed by an equal or greater pressure exerted by the basaltic liquid on the trailing edge of the sulfide droplet that tends to push the droplet into the pore. This pressure is exerted by the hydraulic gradient that accompanies the flow of the basaltic liquid out of the compacting rock. If the pressure drop in the basalt from one end of the pore to the other is not greater than the excess pressure exerted on the interior of the sulfide drop by the capillary force at the point of the tightest constriction in the pore throat, then it will not be able to pass through the pore.

The maximum possible hydraulic gradient ΔP_b within the basalt along the length of the compacting system during compaction-driven melt extraction is provided by the buoyancy of the melt with respect to the solid framework,

$$\Delta P_b = \Delta\rho gH \tag{10}$$

where $\Delta\rho$ is the difference in density between the silicate melt and the solid framework, g is the acceleration due to gravity, and H is the height of the system. The pressure drop will be diminished to the extent that compaction is retarded by the much greater viscosity of the solid matrix than that of the silicate melt. To a first approximation to an absolute upper limiting value, therefore, the pressure drop from one end to the other of a given pore throat should scale with $\Delta\rho gh$ where h is the vertical length of the pore throat. Combining Eqs. (9) and (10) at the scale of the individual pore, we find that at the critical hydraulic gradient to permit transport of the sulfide droplet through the pore,

$$\frac{2\gamma_{SF}}{R_o} - \frac{2\gamma_{SF}}{R_{min}} = \Delta\rho gh \tag{11}$$

Substituting values of 0.5 J m^{-2} for γ_{SF}, 10^{-4} m for R_o, and 10^{-5} m for R_{min}, we find that the capillary pressure is of the order of 10^4 Pa, whereas for a density difference of 1000 kg m^{-3}, $g = 10$ ms^{-2}, and pore length $h = 10^{-3}$ m, the driving pressure for droplet transport is only 10 Pa. The pressure tending to drive droplets through constrictions in the porous partially molten rock is therefore at least three orders of magnitude smaller than the retarding capillary pressure. Considering that we have assumed that solid olivine and basaltic liquid have the same viscosity to

arrive at this conclusion, it is clear that if the true viscosity of the compacting solids were used the hydraulic gradient would be many orders of magnitude smaller, making transport of sulfide droplets quantitatively impossible during mantle melting.

The foregoing discussion provides a qualitative argument against the mobilization of immiscible sulfide in ascending silicate melts during the extraction of melt from the mantle if the process is driven by compaction. If pore throats are much larger, as in a newly formed cumulate with high porosity, or if sulfide is present as sufficiently small droplets, these constraints will be lifted and sulfide will be free to migrate.

The crystallization range of sulfide magmas is similar to that of mafic silicate magmas but extends to lower temperatures. Whereas the solidus of most mafic magmatic systems is near 950 °C, the last sulfide melt probably crystallizes at temperatures well below this point, perhaps below 800 °C [25]. It is commonly observed that a sulfide magma has remained effectively contained in a single body over most of its crystallization range, only to be released to form veins and disseminations at very low temperatures when only a tiny fraction of the sulfide remains in the liquid state [26,27].This behavior is consistent with the proposition that sulfide melts are prevented from migrating through silicate rocks as long as even a trace of interstitial silicate melt remains present. Once all of the silicate melt has crystallized, the last remaining sulfide liquid experiences no barrier to its migration and will tend to soak out of the nearly solid sulfide mass and into the surrounding rocks, provided that the dihedral angle of silicate minerals against sulfide melt is less than 60°. Our experience in the laboratory shows abundant evidence that without silicate melt to block its progress, sulfide melt can infiltrate silicate containers, causing impermeable materials like amorphous silica to recrystallize to a porous mass of crystals, and passing right through solid containers along grain boundaries or microfractures.

6. Conclusions

The interfacial tension γ_{SF} between sulfide and silicate melt varies from about 500 to 650 mJ m^{-2},

values much larger than those of interfaces between silicate or oxide minerals and silicate melt. The sulfide–silicate interfacial tension shows no discernable temperature dependence from 1250 to 1325 °C and is a weakly increasing function of the amount of Cu, Ni or O that is added to a base composition corresponding to liquid FeS. The sulfide–silicate interfacial tension is considerably larger than was previously measured in metallurgical slag–matte systems, probably due to the much lower FeO concentrations in the basalt than in typical slags. Densities of sulfide liquids show little dependence on Cu or Ni content, remaining within the range from 4.0 to 4.5 g cm^{-3} over wide ranges in Cu and Ni content, but increase markedly to as high as 5.5 g cm^{-3} in Fe–S–O melt containing 4 wt.% O. Contact angles of sulfide drops immersed in basaltic silicate melt and sitting upon alumina substrates are very large, in the range from 150° to 180°.

We suggest that the nucleation of sulfide droplets from sulfide-saturated silicate magmas may suffer substantial delays due to kinetic hurdles related to the high interfacial energies of small droplets. Once sulfide liquid has formed as a discrete phase, it will tend not to wet silicate or oxide minerals and will therefore be impeded from migrating through semi-solid silicate rocks. Sulfide will only be free to travel along fractures and silicate grain boundaries or triple grain edges at temperatures below the solidus temperature of silicate melt. As long as a body of sulfide melt is enclosed by silicate rocks that contain traces of silicate melt along their grain boundaries, sulfide liquid will tend to remain confined to the places where it originally came to rest. The commonly observed dispersion of very late sulfide liquid from bodies of massive sulfide into silicate host rocks may be a consequence of the final solidification of the silicate rocks and the resulting ability of sulfide liquid to permeate the grain-boundary porosity of the melt-free silicate rock.

Acknowledgements

References

[1] J.E. Mungall, Kinetic controls on the partitioning of trace elements between silicate and sulphide liquids, J. Petrol. 43 (2002) 749–768.

[2] S.W. Ip, J.M. Toguri, Surface and interfacial tension of the Ni–Fe–S, Ni–Cu–S, and fayalite slag systems, Metal. Trans. 24B (1993) 657–668.

[3] M. Kucharski, S.W. Ip, J.M. Toguri, The surface tension and density of Cu$_2$S, FeS, Ni$_3$S$_2$ and their mixtures, Can. Metal. Quart. 33 (1994) 197–203.

[4] H.St.C. O'Neill, J.A. Mavrogenes, The sulfide capacity and the sulfur content at sulfide saturation of silicate melts at 1400 °C and 1 bar, J. Petrol. 43 (2002) 1049–1087.

[5] C.L. Peach, E.A. Mathez, R.R. Keays, Sulfide melt–silicate melt distribution coefficients for noble metals and other chalcophile elements as deduced from MORB: implications for partial melting, Geochim. Cosmochim. Acta 54 (1990) 3379–3389.

[6] J.E. Mungall, Interfacial tension in miscible two-fluid systems with linear viscoelastic rheology, Phys. Rev. Lett. 73 (1994) 288–291.

[7] P.G. de Germes, Wetting: statics and dynamics, Rev. Modern Phys. 57 (1985) 827–863.

[8] Y. Rotenberg, L. Boruvka, A.W. Neumann, Determination of suface tension and contact angle from the shapes of axisymmetric fluid interfaces, J. Colloid Interface Sci. 93 (1983) 169–183.

[9] E. Dowty, Crystal growth and nucleation theory and the numerical simulation of igneous crystallization, in: R.B. Hargraves (Ed.), Physics of Magmatic Processes, Princeton University Press, 1980, pp. 419–485.

[10] J.W.P. Schmelzer, A.R. Gokhman, V.M. Fokin, Dynamics of first-order phase transitions in multicomponent systems: a new theoretical approach, J. Colloid Interface Sci. 272 (2004) 109–133.

[11] J. Deubener, M.C. Weinberg, Crystal-liquid surface energies from transient nucleation, J. Non-Cryst. Solids 23 1 (1998) 143–151.

[12] L.G. Gránásy, Y.T. Pusztai, P.F. James, Interfacial properties deduced from nucleation experiments: a Cahn–Hilliard analysis, J. Chem. Phys. 117 (2002) 6157–6168.

[13] J.E. Mungall, Late-stage sulfide liquid mobility in the Main Mass of the Sudbury Igneous Complex; examples from the Victor Deep, McCreedy East and Trillabelle deposits, Econ. Geol. 97 (2002) 1563–1576.

[14] W.D. Maier, S.-J. Barnes, Platinum-group elements in silicate rocks of the Lower, Critical and Main Zones at Union Section, Western Bushveld Complex, J. Petrol. 40 (1999) 1647–1671.

[15] C. Bockrath, A. Holzheid, C. Ballhaus, Fractionation of platinum group elements is not controlled by sulfide/silicate partition coefficients, EUG Nice Prog. Abstr. EAE03-A-11634 156 April 6–11, 2003.

[16] D. McKenzie, The generation and compaction of partially molten rock, J. Petrol. 25 (1984) 713–765.

[17] W.G. Minarik, F.J. Ryerson, E.B. Watson, Textural entrapment of core-forming melts, Science 272 (1996) 530–533.

[18] M.C. Shannon, C.B. Agee, High pressure constraints on percolative core formation, Science 280 (1996) 1059–1061.

[19] G.A. Gaetani, T.L. Grove, Wetting of mantle olivine by sulfide melt: implications for Re/Os ratios in mantle peridotite and late-stage core formation, Earth Planet. Sci. Lett. 169 (1999) 147–163.

[20] L.A. Rose, J.M. Brenan, Wetting properties of Fe–Ni–Cu–Co–O–S melts against olivine: implications for sulfide mobility, Econ. Geol. 96 (2001) 145–157.

[21] J.M. Brenan, L.A. Rose, Experimental constraints on the wetting of chromite by sulfide liquid, Can. Mineral. 40 (2002) 113–126.

[22] T.M. Tharp, R.R. Loucks, R.O. Sack, Modeling compaction of olivine cumulates in the Muskox intrusion, Am. J. Sci. 298 (1998) 758–790.

[23] G. Schubert, D.L. Turcotte, P. Olson, Mantle Convection in the Earth and Planets, Cambridge University Press, 2001, 940 pp.

[24] H.E. Dawson, P.V. Roberts, Influence of viscous, gravitational, and capillary forces on DNAPL saturation, Ground Water 35 (1997) 261–269.

[25] C. Ballhaus, M. Tredoux, A. Späth, Phase relations in the Fe–Ni–Cu–PGE–S system at magmatic temperature and application to the massive sulphide ores of the Sudbury Igneous Complex, J. Petrol. 42 (2001) 1911–1926.

[26] J.E. Mungall, D.R. Andrews, L. Cabri, P.J. Sylvester, M. Tubrett. Partitioning of Cu, Ni, Au and platinum-group elements between monosulfide solid solution and sulfide melt under controlled oxygen and sulfur fugacities, Geochim. Cosmochim. Acta (in press) (doi:10.1016/j.gca.2004.11.025).

[27] C. Li, A.J. Naldrett, C.J.A. Coats, P. Johannessen, Platinum, palladium, gold and copper-rich stringers at Strathcona Mine, Sudbury: their enrichment by fractionation of a sulfide liquid, Econ. Geol. 87 (1992) 1584–1596.